Communication

Not peer-reviewed version

Genome-Wide Selection Signals of the Min Pig Indicate That Genes Related to Fat and Energy Metabolism Play a Crucial Role in Responding to Cold Stress

Wentao Wang , Liang Wang , Haoyuan Zhang , Yaolong Liu , Guangxin E * , Dongjie Zhang *

Posted Date: 19 May 2025

doi: 10.20944/preprints202505.1448.v1

Keywords: min pig; cold adaptability; energy metabolism; fatty acid synthesis

 doi:10.20944/preprints202505.1448.v1

Communication

Genome-Wide Selection Signals of the Min Pig Indicate That Genes Related to Fat and Energy Metabolism Play a Crucial Role in Responding to Cold Stress

Wentao Wang [1], Liang Wang [1], Haoyuan Zhang [2], Yaolong Liu [2], Guangxin E [2,*] and Dongjie Zhang [1,*]

[1] Institute of Animal Husbandry, Heilongjiang Academy of Agricultural Sciences, Harbin 150086, China
[2] College of Animal Science and Technology, Southwest University, Chongqing 400715, China
* Correspondence: eguangxin@126.com (G.E.); djzhang8109@163.com

Simple Summary: This study identified key candidate genes for cold adaptation in Min pigs through genome-wide selection sweep analysis (GWSA), revealing a large number of genes related to fat synthesis and energy metabolism that were selected in Min pigs, such as *AKT3*, *PRKG1*, *CREB3L3*, etc. This suggests that these genes enhance the energy supply and body temperature maintenance ability of Min pigs in low-temperature environments.

Abstract: As a typical northeast indigenous pig breed of China, the Min Pig (MZ) with excellent cold adaptability by long-term natural selection. This provides a natural animal model for understanding the genetic basis of cold exposure adaptation in pigs. In this study, a genome-wide selective sweep analysis (GWSA) of 30 MZ and 42 public pig genomes without cold resistant adaptability was performed to identify candidate genes (CDGs) of cold stress tolerance, based on genome-wide SNP dataset. The results revealed that a total 226 interacting CDGs were obtained from 5% windows of FST (≥ 0.412596), θπ ratio (≥ 2.125852484) and XP-CLR (≥ 22.08201682). 68 of them were enriched in 183 KEGG pathways, with 24 KEGG pathways significantly enriched (corrected-$P < 0.05$), including the cGMP-PKG and PI3K-Akt signaling pathway, etc. Specifically, numerous CDGs (e.g., *AKT3*, *PRKG1*, *CREB3L3*, *ACSF3*, and *NDUFS7*) were enriched in pathways related to fat synthesis and energy metabolism, such as Fatty acid biosynthesis, Carbohydrate digestion and absorption, Adipocytokine signaling pathway, Regulation of lipolysis in adipocytes and Insulin resistance, etc. In summary, this study not only identified relative CDGs underlying the adaptive genetic basis of cold stress resistance in MZ, but also provided a scientific foundation for the molecular breeding of environmental adaptability in pig.

Keywords: Min Pig; cold adaptability; energy metabolism; fatty acid synthesis

1. Introduction

Pork, as one of the most consumed meats globally, is a significant source of protein and nutrients in the human diet [1]. Indigenous pig breeds hold unique value in the pig industry and breeding, as they have undergone long-term natural selection and adaptive evolution, enabling efficient production under specific environmental conditions and providing valuable genetic resources for the sustainable development of the global pig industry. The Min Pig (MZ), a typical representative of Chinese indigenous pig breeds, has developed distinct genetic traits through prolonged natural selection and domestication, particularly excelling in cold adaptability [2].

 doi:10.20944/preprints202505.1448.v1

With the completion of the Swine Genome Project, breeders worldwide have successfully identified multiple key genes influencing economic traits in pigs using high-density genotyping and resequencing technologies. For instance, genes related to growth rate (e.g., *FASN*, *ELOVL6*, *SSC7*, *SSC2*) [3–5], lean meat percentage (e.g., *NCK2*, *ACSL1*, *PPARG*) [6–8] , meat quality (e.g., *GHRHR*, *SSC18*, *CDYL2*) [7,9,10] , and litter size (e.g., *IGFBP2*, *UBE3A*, *FAM135B*) have been pinpointed [11–13].

In recent years, a series of candidate genes related to environmental adaptability in pigs have been identified. For example, *FBN1* was confirmed that closely related to skin thickness in pigs and may involve in their environmental adaptability [14,15]. Previous studies identified several candidate genes of physiological responses of pigs under heat stress, including *GHR*, *TEAD4*, *NNT*, *ERBB4*, *FKBP1B*, and *NFATC2* [16]. Additionally, current study indicated that the haplotypes of the *BTF3* gene significantly differ between Chinese and Western pig breeds, influencing fat tissue formation by promoting adipocyte proliferation and regulating intramuscular fat deposition [17]. Furthermore, the upregulation of glucose metabolism-related genes (e.g., *ACSS1*, *HK3*, *PGM2*, *PCK1*) under cold stress environments was confirmed to enhance glycolysis, gluconeogenesis, and glycogenolysis, increasing energy production to counteract cold exposure [18]. In this study, a genome-wide selective sweep analysis (GWSA) of MZ was performed to systematically identify selected genes relative to their cold adaptability, which will be helpful to deepen the genetic basis understanding of cold adaptability in pigs.

2. Materials and Methods

In this study, total of 30 MZ blood samples, with no familial relationships within three generavation farm in Lanxi City, Heilongjiang Province of China (E 126°16′, N 46°15′). Genomic DNA was extracted using TaKaRa MiniBEST Universal Genomic DNA Extraction Kit Ver.5.0 (Takara, Japan). Sequencing libraries were constructed by Annoroad® Universal DNA Library Preparation Kit v2.0 (Illumina®, San Diego, CA, USA) and sequenced on the BGISEQ-500 platform (Beijing Genomics Institute, China) with a sequencing depth of ~10× per individual. Additionally, the publicly available genomic data of 42 samples from 7 breeds without cold adaptability were obtained from the Sequence Read Archive (SRA) database (Table S1) as control group for subsequent GWSA. These populations included 3 indigenous pigs in southern China, such as Chenghua (CH, n=5), Rongchang (RC, n=7) and Meishan (MS, n=5) and 4 commercial breeds, such as Duroc (DL, n=6), Yorkshire (YK, n=7), Landrace (CB, n=5), and French Large White (DB, n=7).

Integration with publicly available data and 30 MZ genome re-sequence data produced from this study, a total of 1566.8 GB of raw sequencing data were obtained. The raw data were quality-controlled and filtered using Fastp (v0.23.4) with default parameters to obtain high-quality clean reads (HQRs). Subsequently, all HQRs were aligned to the pig reference genome (GCF_000003025.6, *Sscrofa* 11.1) using bwa-mem2 (v2.2.1) for further analysis. Single nucleotide polymorphisms (SNPs) were identified using the HaplotypeCaller module in the Genome Analysis Toolkit (GATK, version 4.5.0.0), and variant quality filtering was performed using the VariantFiltration module (McKenna et al. 2010). The filtering criteria were set as follows: quality depth (QD) <2.0, variant quality (QUAL) <30.0, strand bias ratio (SOR) >3.0, Fisher's exact test (FS) >60.0, mapping quality (MQ) <40.0, mapping quality rank sum test (MQRankSum) <-12.5, and read position rank sum test (ReadPosRankSum) <-8.0. Further filtering of autosomal SNPs was performed using vcftools (v0.1.16) [19] with the following parameters: only biallelic variants retained (--min-alleles 2 --max-alleles 2), genotype missing rate <0.05 (--max-missing 0.95), and minimum allele frequency > 0.05, (--maf 0.05). Finally, candidate SNPs were functionally annotated using Annovar software [20].

The GWSA was conducted on MZ (case) and other non-cold-adapted breeds (control) using 3 statistical algorithms: fixation index (FST) [21], nucleotide diversity difference ($\theta\pi$ ratio) [22] , and cross-population composite likelihood ratio test (XP-CLR) [23]. The analysis of these parameters was estimated with a sliding window of 40 kb and a step size of 20 kb. The top 5% of windows (thresholds set as follows: FST≥ 0.412596, $\theta\pi$ ratio≥ 2.125852484, and XP-CLR≥ 22.08201682) were selected from

 doi:10.20944/preprints202505.1448.v1

each parameter, and regions overlapping across all three methods were considered candidate selective regions (CSRs). The candidate genes (CDGs) were defined as the genes overlapped in above CSRs. Subsequently, the Kyoto Encyclopedia of Genes and Genomes (KEGG) enrichment analyses were performed on CDGs using online tool KOBAS (http://kobas.cbi.pku.edu.cn/), with a significance threshold set at a corrected *P*-value <0.05.

3. Results and Discussion

A total of 1,566.8 GB of raw sequencing data were obtained. Across all 72 individuals, 60,652,730 SNPs were identified, and 23,991,936 high-quality SNPs were retained for subsequent analysis after quality control. The selection signal results indicated that the windows with the highest FST values were located on chromosomes CHR4 and CHR5 (Figure 1A), while the windows with the greatest θπ ratio differences were found on CHR4 and CHR8 (Figure 1B). The windows with the highest XP-CLR values were located on CHR4 and CHR15 (Figure 1C). Based on the intersection of top 5% windows from these three parameters, total 58,771 SNPs were obtained from 357 intersected windows, which located in exonic, intronic, 3'UTR, 5'UTR, and upstream/downstream regions. Finally, total 226 candidate genes were identified originating from 357 intersecting windows.

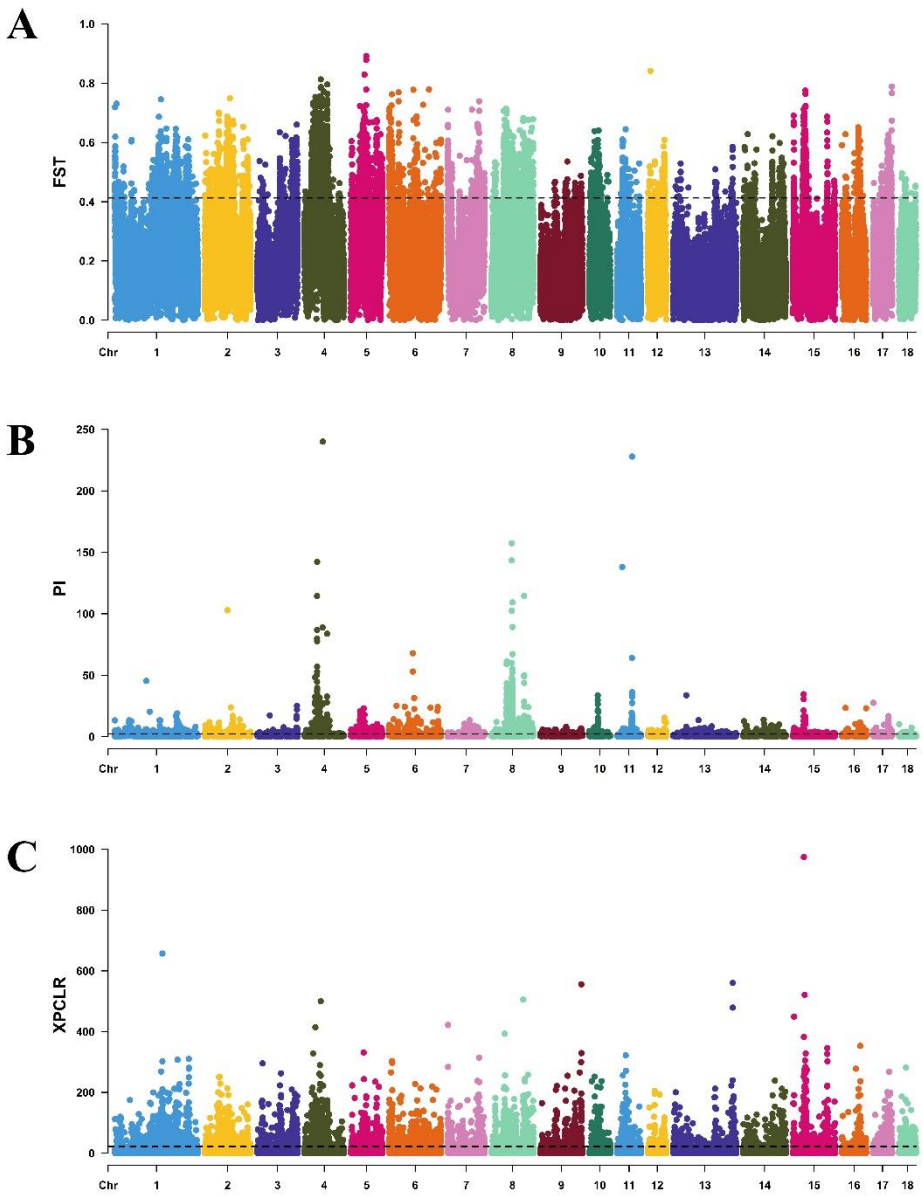

 doi:10.20944/preprints202505.1448.v1

Figure 1. Manhattan plots of genome-wide selection sweep analysis for cold adaptation in pigs. (A) Manhattan plots of FST analysis for cold adaptation in pigs. (B) Manhattan plots of θπ ratio analysis for cold adaptation in pigs. (C) Manhattan plots of XP-CLR analysis for cold adaptation in pigs.

Additionally, gene functional annotation results revealed that 68 of 226 CDGs were enriched in 183 KEGG pathways, with 24 KEGG pathways significantly enriched (corrected-$P < 0.05$, Table 1), including the cGMP-PKG signaling pathway (*NFATC2, MAP2K2, MYLK4, CREB3L3, AKT3, PRKG1*), PI3K-Akt signaling pathway (*ERBB4, CREB3L3, MAP2K2, GNG7, AKT3, MDM2, ANGPT1, BDNF*), and Kaposi sarcoma-associated herpesvirus infection (*NFATC2, MAP2K2, PREX1, GNG7, AKT3, LYN*). Furthermore, numerous CDGs (e.g., *AKT3, PRKG1, CREB3L3, ACSF3, and NDUFS7*) were enriched in pathways related to fat synthesis and energy metabolism, such as Fatty acid biosynthesis, Carbohydrate digestion and absorption, Adipocytokine signaling pathway, Regulation of lipolysis in adipocytes, Glucagon signaling pathway, Insulin resistance, and Thermogenesis, etc.

Table 1. Significantly enriched KEGG pathways of candidate genes.

KEGG Pathways	Enrishment Genes	Corrected *P*-Value
cGMP-PKG signaling pathway	*NFATC2, MAP2K2, MYLK4, CREB3L3, AKT3, PRKG1*	0.0089
PI3K-Akt signaling pathway	*ERBB4, CREB3L3, MAP2K2, GNG7, AKT3, MDM2, ANGPT1, BDNF*	0.0124
Kaposi sarcoma-associated herpesvirus infection	*NFATC2, MAP2K2, PREX1, GNG7, AKT3, LYN*	0.0126
Ubiquitin mediated proteolysis	*APC2, RCHY1, MDM2, UBE2C, PIAS4*	0.0179
Human T-cell leukemia virus 1 infection	*CDKN2B, NFATC2, CREB3L3 , MAP2K2, AKT3, APC2*	0.0179
Human cytomegalovirus infection	*NFATC2, CREB3L3, MAP2K2, GNG7, AKT3, MDM2*	0.0192
B cell receptor signaling pathway	*MAP2K2, NFATC2, AKT3, LYN*	0.0192
Ras signaling pathway	*EXOC2, GNG7, MAP2K2, AKT3, BDNF, ANGPT1*	0.0204
Cellular senescence	*CDKN2B, MAP2K2, NFATC2, AKT3, MDM2*	0.0223
Hepatitis B	*CREB3L3, NFATC2, AKT3, APAF1, MAP2K2*	0.0227
Fc gamma R-mediated phagocytosis	*PIP5K1C, DOCK2, LYN, AKT3*	0.0234
Bladder cancer	*MAP2K2, MDM2, DAPK3*	0.0245
Prostate cancer	*CREB3L3, MDM2, AKT3, MAP2K2*	0.0248
Chemokine signaling pathway	*DOCK2, GNG7, LYN, AKT3, PREX1*	0.0327
Thyroid hormone signaling pathway	*MAP2K2, MDM2, AKT3, MED13*	0.0369
Yersinia infection	*PIP5K1C, MAP2K2, NFATC2, AKT3*	0.0379
Platelet activation	*LYN, AKT3, PRKG1, MYLK4*	0.0379
VEGF signaling pathway	*MAP2K2, NFATC2, AKT3*	0.0379
Regulation of actin cytoskeleton	*MOS, MAP2K2, PIP5K1C, MYLK4, MYH10*	0.0388
Long-term depression	*MAP2K2, LYN, PRKG1*	0.0388
Relaxin signaling pathway	*CREB3L3, GNG7, AKT3, MAP2K2*	0.0388

 doi:10.20944/preprints202505.1448.v1

FoxO signaling pathway	*CDKN2B, MAP2K2, MDM2, AKT3*	0.0391
Apelin signaling pathway	*MAP2K2, MYLK4, AKT3, GNG7*	0.0424
Fc epsilon RI signaling pathway	*MAP2K2, LYN, AKT3*	0.0457

As well-known, fat plays a crucial role in resisting low-temperature environments, serving as a key substance for providing energy, maintaining body temperature, and enhancing cold stress resistance. This study identified a large number of genes related to fat metabolism and synthesis that are under selection in MZ. For example, *ACSF3* is a malonyl-CoA synthetase involved in the synthesis of fatty acids in mammalian mitochondria [24], and its activity also affects the malonylation level of *ACOT7*, thereby regulating fat content in animal muscles [25,26]. ATP6V1H is the H subunit of the V1 subunit of V-ATPase, participating in the assembly and functional regulation of V-ATPase, which is crucial for maintaining cellular acid-base balance and various physiological processes [27]. Research has found that the absence of *ATP6V1H* increases endoplasmic reticulum stress in pancreatic β-cells and exacerbates glucose tolerance impairment caused by fatty acids [28]. This indicates that *ATP6V1H* plays a key role in cellular metabolism and stress response, and its dysfunction may affect the body's adaptation to cold stress. *NMRK2* is a muscle-specific β1 integrin-binding protein that activates the *SIRT1* pathway by increasing NAD+ levels, thereby promoting fatty acid oxidative metabolism and enhancing cold resistance in animals [29,30], and it is potentially related to the development and regulation of goat adipose tissue [31]. The *PIP5K1C* gene encodes phosphatidylinositol-4-phosphate 5-kinase, which is involved in phospholipid metabolism and promotes the synthesis of diacylglycerol (DAG) and phosphatidylinositol (PI) [32]. The activity of *PIP5K1C* affects cell signaling pathways, especially those related to cell migration and signaling [33,34]. Previous studies have confirmed that the absence of *PIP5K1C* in adipocytes reduces the phosphorylation levels of PI3K and AKT, thereby inhibiting the activity of the PI3K/AKT signaling pathway and promoting cell apoptosis [35] .

Moreover, *GAMT,* as a crucial enzyme in the synthesis of creatine, regulates the creatine-phosphocreatine system to maintain high-energy phosphate reserves, providing rapid ATP supply to muscle and nerve tissues under low-temperature conditions [36] . Research indicates that *GAMT* deficiency decreases the efficiency of muscle energy metabolism, exacerbating metabolic imbalances caused by cold stress [37]. Its involvement in creatine metabolism indirectly enhances thermogenic capacity by modulating mitochondrial function, thereby improving cold adaptation [38] . The *AMPD3* activates the *AMPK* pathway by regulating the AMP/ATP ratio, promoting fatty acid oxidation and thermogenic metabolism[39,40]. Overexpression of *AMPD3* was also reported to increase mitochondrial oxygen consumption rates in muscles[41].Studies suggest that overexpression of *CREB3L3* enhances lipolysis, ketogenesis, and insulin sensitivity, increasing energy expenditure and improving metabolic indicators, revealing its critical regulatory role in energy metabolism and thermogenic processes[42–44].

PRKG1, as a cGMP-dependent protein kinase, was suggested to play a critical role in the vasoconstrictive response induced by cold exposure. For example, study indicates that *PRKG1* regulates the localization and function of the Rho A protein through its phosphorylation, to decreasing the phosphorylation of myosin light chains, thereby promoting vasodilation [45]. Additionally, *PRKG1* facilitates the hydrolysis of triglycerides to release free fatty acids and glycerol[46]. Calcium-dependent neutral proteases, such as Calpain-1, also play a crucial role in the regulation of mitochondrial function and cellular stress responses, with their activity being associated with mitochondrial calcium overload. Inhibiting Calpain-1 has been shown to enhance mitochondrial function and reduce cellular damage[47], thereby maintaining thermogenic efficiency. *NDUFS7* is the core catalytic subunit of mitochondrial complex I (NADH dehydrogenase), directly involved in the electron transfer from NADH to ubiquinone [48]. It was reported that an inhibitor (DX2-201) targets *NDUFS7* and inhibits mitochondrial function and oxidative phosphorylation by suppressing the activity of complex I [49]. Furthermore, the deficiency of *NDUFS7* leads to a decreased cell proliferation, increased cell death, and increased susceptibility to oxidative stress [50]. It is worth

 doi:10.20944/preprints202505.1448.v1

noting that studies have shown that exposure of animals with constant temperature to low environmental temperatures is associated with oxidative stress in various body tissues [51].

ACOT8 (Acyl-CoA Thioesterase 8) is a member of the acyl-CoA thioesterase superfamily and acts as a peroxisomal acyl-CoA thioesterase capable of hydrolyzing various acyl-CoA substrates[52]. Study indicates that *ACOT8* facilitates the conversion of acetyl-CoA into acetate and CoA, thereby promoting the reutilization of CoA and supporting the ongoing process of fatty acid oxidation (FAO) during energy stress. Furthermore, *ACOT8* is upregulated enhancing the function of *HMGCS2* (3-Hydroxy-3-Methylglutaryl-CoA Synthase 2) to promote ketogenesis, thus supplying fuel to extrahepatic tissues and enhancing the body's cold tolerance[53]. Lmpad1 is a Golgi-resident protein that regulates Golgi morphology and vesicular transport[54]. Under low-temperature conditions, *IMPAD1* may maintain Golgi function, facilitating the glycosylation of mitochondrial-related enzymes, which optimizes ATP production efficiency, decrease ROS levels and alleviates energy shortages [55].

B4GALT5 (β-1,4-galactosyltransferase 5) belongs to the β-4-galactosyltransferase gene family associated with the Golgi apparatus and plays a crucial role in the biosynthesis of glycosphingolipids and glycans. It primarily catalyzes the attachment of galactose to glycosphingolipid or glycoprotein receptors, such as GlcNAc, Glc, and Xyl, through β-1,4-glycosidic bonds[56]. Studies indicate that *B4GALT5* is present not only on the cell surface but also within the Golgi complex, where it functions as an adhesion molecule involved in matrix interactions, cellular spreading and migration, and signal transduction cascades[57,58]. This suggests that *B4GALT5* may enhance the cold stability of cell membranes and adhesion structures through glycosylation modifications, thereby promoting the cellular migratory capacity associated with cold injury repair and optimizing the efficiency of stress signaling pathways.

4. Conclusion

In this study, a series of genes involved in fat metabolism, energy homeostasis, and mitochondrial function that are under selection in MZ were confirmed by GWSA analysis. These findings not only deepen our understanding to genetic basis of cold adaptation, but also provide support for further development of environmental adaptation breeding markers for pigs.

Supplementary Materials: The following supporting information can be downloaded at the website of this paper posted on Preprints.org. Table S1 Sample information for identifying adaptability of Min Pigs to cold environment. Table S2 Candidate selective regions related to the cold adaptability of Min Pigs in FST. Table S3 Candidate selective regions related to the cold adaptability of Min Pigs in θπ ratio. Table S4 Candidate selective regions related to the cold adaptability of Min Pigs in XP-CLR. Table S5 KEGG pathway enrichment results of candidate genes

Author Contributions: Conceptualization, Dong-Jie Zhang, and Wen-Tao Wang; Data curation, Wen-Tao Wang and Yao-Long Liu; Funding acquisition, Dong-Jie Zhang; Methodology, Wen-Tao Wang, Liang Wang and Hao-Yuan Zhang; Writing–original draft, Wen-Tao Wang. All authors have read and agreed to the published version of the manuscript.

Funding: This work was supported by the National Natural Science Foundation of China (32172696) and Science and Technology Innovation Project of Heilongjiang Academy of Agriculture Sciences (CX22JQ03).

Institutional Review Board Statement: The experimental procedures of this study were authorized by the Ethics Committee of Institute of Animal Husbandry, Heilongjiang Academy of Agricultural Sciences (Approval Number: IAH-202407).

Informed Consent Statement: Not applicable.

 doi:10.20944/preprints202505.1448.v1

Data Availability Statement: The data of whole genome sequencing has been deposited at NCBI database with the accession number PRJNA1258739.

Acknowledgments: Not applicable.

Conflicts of Interest: The authors declare that there are no conflicts of interest between them with respect to publishing this paper.

References

1. Drewnowski, A. Perspective: The place of pork meat in sustainable healthy diets; *Adv Nutr* **2024**, 15(5): 100213. DOI 10.1016/j.advnut.2024.100213
2. Zhang, D.; Wang, L.; Ma, S.; Ma, H.; Liu, D. Characterization of pig skeletal muscle transcriptomes in response to low temperature; *Vet Med Sci* **2023**, 9(1): 181-190. DOI 10.1002/vms3.1025。
3. Guo, Y.; Huang, Y.; Hou, L.; Ma, J.; Chen, C.; Ai, H.; Huang, L.; Ren, J. Genome-wide detection of genetic markers associated with growth and fatness in four pig populations using four approaches; *Genet Sel Evol* **2017**, 49(1): 21. DOI 10.1186/s12711-017-0295-4。
4. Wang, M.; Zhang, X.; Kang, L.; Jiang, C.; Jiang, Y. Molecular characterization of porcine necd, snrpn and ube3a genes and imprinting status in the skeletal muscle of neonate pigs; *Mol Biol Rep* **2012**, 39(10): 9415-9422. DOI 10.1007/s11033-012-1806-6。
5. Zhang, Y.; Zhang, J.; Gong, H.; Cui, L.; Zhang, W.; Ma, J.; Chen, C.; Ai, H.; Xiao, S.; Huang, L.; Yang, B. Genetic correlation of fatty acid composition with growth, carcass, fat deposition and meat quality traits based on gwas data in six pig populations; *Meat Sci* **2019**, 150: 47-55. DOI 10.1016/j.meatsci.2018.12.008。
6. Passols, M.; Llobet-Cabau, F.; Sebastià, C.; Castelló, A.; Valdés-Hernández, J.; Criado-Mesas, L.; Sánchez, A.; Folch, J.M. Identification of genomic regions, genetic variants and gene networks regulating candidate genes for lipid metabolism in pig muscle; *animal* **2023**, 17(12): 101033. DOI 10.1016/j.animal.2023.101033。
7. Wang, H.; Wang, X.; Li, M.; Sun, H.; Chen, Q.; Yan, D.; Dong, X.; Pan, Y.; Lu, S. Genome-wide association study of growth traits in a four-way crossbred pig population; *Genes (Basel)* **2022**, 13(11). DOI 10.3390/genes13111990。
8. Xu, J.; Wang, C.; Jin, E.; Gu, Y.; Li, S.; Li, Q. Identification of differentially expressed genes in longissimus dorsi muscle between wei and yorkshire pigs using rna sequencing; *Genes Genomics* **2018**, 40(4): 413-421. DOI 10.1007/s13258-017-0643-3。
9. Hérault, F.; Damon, M.; Cherel, P.; Le Roy, P. Combined gwas and ldla approaches to improve genome-wide quantitative trait loci detection affecting carcass and meat quality traits in pig; *Meat Science* **2018**, 135: 148-158. DOI 10.1016/j.meatsci.2017.09.015。
10. Ibragimov, E.; Pedersen, A.; Sloth, N.; Fredholm, M.; Karlskov-Mortensen, P. Identification of a novel qtl for lean meat percentage using imputed genotypes; *Animal Genetics* **2024**, 55: n/a-n/a. DOI 10.1111/age.13442。
11. An, S.M.; Hwang, J.H.; Kwon, S.; Yu, G.E.; Park, D.H.; Kang, D.G.; Kim, T.W.; Park, H.C.; Ha, J.; Kim, C.W. Effect of single nucleotide polymorphisms in igfbp2 and igfbp3 genes on litter size traits in berkshire pigs; *Anim Biotechnol* **2018**, 29(4): 301-308. DOI 10.1080/10495398.2017.1395345。
12. Sironen, A.I.; Uimari, P.; Serenius, T.; Mote, B.; Rothschild, M.; Vilkki, J. Effect of polymorphisms in candidate genes on reproduction traits in finnish pig populations; *J Anim Sci* **2010**, 88(3): 821-827. DOI 10.2527/jas.2009-2426。
13. Spitschak, M.; Hoeflich, A. Potential functions of igfbp-2 for ovarian folliculogenesis and steroidogenesis; *Front Endocrinol (Lausanne)* **2018**, 9: 119. DOI 10.3389/fendo.2018.00119。
14. Cross, A.J.; Keel, B.N.; Brown-Brandl, T.M.; Cassady, J.P.; Rohrer, G.A. Genome-wide association of changes in swine feeding behaviour due to heat stress; *Genet Sel Evol* **2018**, 50(1): 11. DOI 10.1186/s12711-018-0382-1。
15. Wang, Y.; Gou, Y.; Yuan, R.; Zou, Q.; Zhang, X.; Zheng, T.; Fei, K.; Shi, R.; Zhang, M.; Li, Y.; Gong, Z.; Luo, C.; Xiong, Y.; Shan, D.; Wei, C.; Shen, L.; Tang, G.; Li, M.; Zhu, L.; Li, X.; Jiang, Y. A chromosome-level genome of chenghua pig provides new insights into the domestication and local adaptation of pigs; *Int J Biol Macromol* **2024**, 270(Pt 1): 131796. DOI 10.1016/j.ijbiomac.2024.131796。

 doi:10.20944/preprints202505.1448.v1

16. Kim, K.S.; Seibert, J.T.; Edea, Z.; Graves, K.L.; Kim, E.S.; Keating, A.F.; Baumgard, L.H.; Ross, J.W.; Rothschild, M.F. Characterization of the acute heat stress response in gilts: Iii. Genome-wide association studies of thermotolerance traits in pigs; *J Anim Sci* **2018**, 96(6): 2074-2085. DOI 10.1093/jas/sky131。
17. Li, D.; Wang, Y.; Yuan, T.; Cao, M.; He, Y.; Zhang, L.; Li, X.; Jiang, Y.; Li, K.; Sun, J.; Lv, G.; Su, G.; Wang, Q.; Pan, Y.; Li, X.; Jiang, Y.; Yang, G.; Groenen, M.A.M.; Derks, M.F.L.; Ding, R.; Ding, X.; Yu, T. Pangenome and genome variation analyses of pigs unveil genomic facets for their adaptation and agronomic characteristics; *Imeta* **2024**, 3(6): e257. DOI 10.1002/imt2.257
18. Zhang, D.; Ma, S.; Wang, L.; Ma, H.; Wang, W.; Xia, J.; Liu, D. Min pig skeletal muscle response to cold stress; *PLoS One* **2022**, 17(9): e0274184. DOI 10.1371/journal.pone.0274184.
19. Danecek, P.; Auton, A.; Abecasis, G.; Albers, C.A.; Banks, E.; DePristo, M.A.; Handsaker, R.E.; Lunter, G.; Marth, G.T.; Sherry, S.T.; McVean, G.; Durbin, R. The variant call format and vcftools; *Bioinformatics* **2011**, 27(15): 2156-2158. DOI 10.1093/bioinformatics/btr330.
20. Wang, K.; Li, M.; Hakonarson, H. Annovar: Functional annotation of genetic variants from high-throughput sequencing data; *Nucleic Acids Res* **2010**, 38(16): e164. DOI 10.1093/nar/gkq603.
21. Weir, B.S.; Cockerham, C.C. Estimating f-statistics for the analysis of population structure; *Evolution* **1984**, 38(6): 1358-1370. DOI 10.1111/j.1558-5646.1984.tb05657.x.
22. Luo, W.; Luo, C.; Wang, M.; Guo, L.; Chen, X.; Li, Z.; Zheng, M.; Folaniyi, B.S.; Luo, W.; Shu, D.; Song, L.; Fang, M.; Zhang, X.; Qu, H.; Nie, Q. Genome diversity of chinese indigenous chicken and the selective signatures in chinese gamecock chicken; *Sci Rep* **2020**, 10(1): 14532. DOI 10.1038/s41598-020-71421-z.
23. Chen, H.; Patterson, N.; Reich, D. Population differentiation as a test for selective sweeps; *Genome Res* **2010**, 20(3): 393-402. DOI 10.1101/gr.100545.109.
24. Witkowski, A.; Thweatt, J.; Smith, S. Mammalian acsf3 protein is a malonyl-coa synthetase that supplies the chain extender units for mitochondrial fatty acid synthesis; *J Biol Chem* **2011**, 286(39): 33729-33736. DOI 10.1074/jbc.M111.291591.
25. He, W.; Fang, X.; Lu, X.; Liu, Y.; Li, G.; Zhao, Z.; Li, J.; Yang, R. Function identification of bovine acsf3 gene and its association with lipid metabolism traits in beef cattle; *Front Vet Sci* **2021**, 8: 766765. DOI 10.3389/fvets.2021.766765.
26. Wang, W.; Ma, C.; Zhang, Q.; Jiang, Y. Tmt-labeled quantitative malonylome analysis on the longissimus dorsi muscle of laiwu pigs reveals the role of acot7 in fat deposition; *J Proteomics* **2024**, 298: 105129. DOI 10.1016/j.jprot.2024.105129.
27. Breton, S.; Brown, D. Regulation of luminal acidification by the v-atpase; *Physiology (Bethesda)* **2013**, 28(5): 318-329. DOI 10.1152/physiol.00007.2013.
28. Yang, S.; Hou, Y.; Zhang, H.; Hao, Y.; Zhang, Y.; Zhao, Z.; Ruan, W.; Duan, X. Atp6v1h deficiency impairs glucose tolerance by augmenting endoplasmic reticulum stress in high fat diet fed mice; *Arch Biochem Biophys* **2022**, 716: 109116. DOI 10.1016/j.abb.2022.109116.
29. Ahmad, F.; Qaisar, R. Nicotinamide riboside kinase 2: A unique target for skeletal muscle and cardiometabolic diseases; *Biochimica et Biophysica Acta (BBA) - Molecular Basis of Disease* **2024**, 1870(8): 167487. DOI 10.1016/j.bbadis.2024.167487.
30. Diguet, N.; Trammell, S.A.J.; Tannous, C.; Deloux, R.; Piquereau, J.; Mougenot, N.; Gouge, A.; Gressette, M.; Manoury, B.; Decaux, J.F.; Lavery, G.G.; Baczkó, I.; Zoll, J.; Garnier, A.; Li, Z.; Brenner, C.; Mericskay, M. Nicotinamide riboside preserves cardiac function in a mouse model of dilated cardiomyopathy; *Circulation* **2018**, 137(21): 2256-2273. DOI 10.1161/circulationaha.116.026099.
31. Zhao, L.; Yang, H.; Li, M.; Xiao, M.; Li, X.; Cheng, L.; Cheng, W.; Chen, M.; Zhao, Y. Global gene expression profiling of perirenal brown adipose tissue whitening in goat kids reveals novel genes linked to adipose remodeling; *J Anim Sci Bio-technol* **2024**, 15(1): 47. DOI 10.1186/s40104-024-00994-w.
32. Heck, J.N.; Mellman, D.L.; Ling, K.; Sun, Y.; Wagoner, M.P.; Schill, N.J.; Anderson, R.A. A conspicuous connection: Structure defines function for the phosphatidylinositol-phosphate kinase family; *Critical reviews in biochemistry and molecular biology* **2007**, 42(1): 15-39. DOI 10.1080/10409230601162752.
33. Qu, M.; Chen, M.; Gong, W.; Huo, S.; Yan, Q.; Yao, Q.; Lai, Y.; Chen, D.; Wu, X.; Xiao, G. Pip5k1c loss in chondrocytes causes spontaneous osteoarthritic lesions in aged mice; *Aging Dis* **2023**, 14(2): 502-514. DOI 10.14336/ad.2022.0828.

 doi:10.20944/preprints202505.1448.v1

34. Wright, B.D.; Loo, L.; Street, S.E.; Ma, A.; Taylor-Blake, B.; Stashko, M.A.; Jin, J.; Janzen, W.P.; Frye, S.V.; Zylka, M.J. The lipid kinase pip5k1c regulates pain signaling and sensitization; *Neuron* **2014**, 82(4): 836-847. DOI 10.1016/j.neuron.2014.04.006.
35. Huang, G.; Yang, C.; Guo, S.; Huang, M.; Deng, L.; Huang, Y.; Chen, P.; Chen, F.; Huang, X. Adipocyte-specific deletion of pip5k1c reduces diet-induced obesity and insulin resistance by increasing energy expenditure; *Lipids Health Dis* **2022**, 21(1): 6. DOI 10.1186/s12944-021-01616-4.
36. Wyss, M.; Kaddurah-Daouk, R. Creatine and creatinine metabolism; *Physiol Rev* **2000**, 80(3): 1107-1213. DOI 10.1152/physrev.2000.80.3.1107.
37. Stockebrand, M.; Sasani, A.; Das, D.; Hornig, S.; Hermans-Borgmeyer, I.; Lake, H.A.; Isbrandt, D.; Lygate, C.A.; Heerschap, A.; Neu, A.; Choe, C.U. A mouse model of creatine transporter deficiency reveals impaired motor function and muscle energy metabolism; *Front Physiol* **2018**, 9: 773. DOI 10.3389/fphys.2018.00773.
38. Wallimann, T.; Dolder, M.; Schlattner, U.; Eder, M.; Hornemann, T.; Kraft, T.; Stolz, M. Creatine kinase: An enzyme with a central role in cellular energy metabolism; *Magma* **1998**, 6(2-3): 116-119. DOI 10.1007/bf02660927.
39. Miller, S.G.; Hafen, P.S.; Law, A.S.; Springer, C.B.; Logsdon, D.L.; O'Connell, T.M.; Witczak, C.A.; Brault, J.J. Amp deamination is sufficient to replicate an atrophy-like metabolic phenotype in skeletal muscle; *Metabolism* **2021**, 123: 154864. DOI 10.1016/j.metabol.2021.154864.
40. Ogawa, T.; Kouzu, H.; Osanami, A.; Tatekoshi, Y.; Sato, T.; Kuno, A.; Fujita, Y.; Ino, S.; Shimizu, M.; Toda, Y.; Ohwada, W.; Yano, T.; Tanno, M.; Miki, T.; Miura, T. Downregulation of extramitochondrial bckdh and its uncoupling from amp deaminase in type 2 diabetic oletf rat hearts; *Physiol Rep* **2023**, 11(4): e15608. DOI 10.14814/phy2.15608.
41. Hong, S.; Zhou, W.; Fang, B.; Lu, W.; Loro, E.; Damle, M.; Ding, G.; Jager, J.; Zhang, S.; Zhang, Y.; Feng, D.; Chu, Q.; Dill, B.D.; Molina, H.; Khurana, T.S.; Rabinowitz, J.D.; Lazar, M.A.; Sun, Z. Dissociation of muscle insulin sensitivity from exercise endurance in mice by hdac3 depletion; *Nat Med* **2017**, 23(2): 223-234. DOI 10.1038/nm.4245.
42. Nakagawa, Y.; Satoh, A.; Yabe, S.; Furusawa, M.; Tokushige, N.; Tezuka, H.; Mikami, M.; Iwata, W.; Shingyouchi, A.; Matsuzaka, T.; Kiwata, S.; Fujimoto, Y.; Shimizu, H.; Danno, H.; Yamamoto, T.; Ishii, K.; Karasawa, T.; Takeuchi, Y.; Iwasaki, H.; Shimada, M.; Kawakami, Y.; Urayama, O.; Sone, H.; Takekoshi, K.; Kobayashi, K.; Yatoh, S.; Takahashi, A.; Yahagi, N.; Suzuki, H.; Yamada, N.; Shimano, H. Hepatic creb3l3 controls whole-body energy homeostasis and improves obesity and diabetes; *Endocrinology* **2014**, 155(12): 4706-4719. DOI 10.1210/en.2014-1113.
43. Ruppert, P.M.M.; Kersten, S. Mechanisms of hepatic fatty acid oxidation and ketogenesis during fasting; *Trends Endocrinol Metab* **2024**, 35(2): 107-124. DOI 10.1016/j.tem.2023.10.002.
44. Wang, W.; Qian, J.; Shang, M.; Qiao, Y.; Huang, J.; Gao, X.; Ye, Z.; Tong, X.; Xu, K.; Li, X.; Liu, Z.; Zhou, L.; Zheng, S. Integrative analysis of the transcriptome and metabolome reveals the importance of hepatokine fgf21 in liver aging; *Genes Dis* **2024**, 11(5): 101161. DOI 10.1016/j.gendis.2023.101161.
45. Zhao, Y.D.; Cai, L.; Mirza, M.K.; Huang, X.; Geenen, D.L.; Hofmann, F.; Yuan, J.X.; Zhao, Y.Y. Protein kinase g-i deficiency induces pulmonary hypertension through rho a/rho kinase activation; *Am J Pathol* **2012**, 180(6): 2268-2275. DOI 10.1016/j.ajpath.2012.02.016.
46. Shi, L.; Lv, X.; Liu, L.; Yang, Y.; Ma, Z.; Han, B.; Sun, D. A post-gwas confirming effects of prkg1 gene on milk fatty acids in a chinese holstein dairy population; *BMC Genet* **2019**, 20(1): 53. DOI 10.1186/s12863-019-0755-7.
47. Liu, X.; Li, M.; Chen, Z.; Yu, Y.; Shi, H.; Yu, Y.; Wang, Y.; Chen, R.; Ge, J. Mitochondrial calpain-1 activates nlrp3 inflammasome by cleaving atp5a1 and inducing mitochondrial ros in cvb3-induced myocarditis; *Basic Res Cardiol* **2022**, 117(1): 40. DOI 10.1007/s00395-022-00948-1.
48. Rhein, V.F.; Carroll, J.; Ding, S.; Fearnley, I.M.; Walker, J.E. Ndufaf5 hydroxylates ndufs7 at an early stage in the assembly of human complex i; *Journal of Biological Chemistry* 2**016**, 291(28): 14851-14860. DOI 10.1074/jbc.M116.734970.

 doi:10.20944/preprints202505.1448.v1

49. Xu, Y.; Xue, D.; Kyani, A.; Bankhead, A.; Roy, J.; Ljungman, M.; Neamati, N. First-in-class nadh/ubiquinone oxidoreductase core subunit s7 (ndufs7) antagonist for the treatment of pancreatic cancer; *ACS Pharmacol Transl Sci* **2023**, 6(8): 1164-1181. DOI 10.1021/acsptsci.3c00069.
50. Chen, J.; Gao, L. Slc7a11-mediated cystine import protects against ndufs7 deficiency-induced cell death in hek293t cells; *Biochem Biophys Res Commun* **2024**, 723: 150178. DOI 10.1016/j.bbrc.2024.150178.
51. Venditti, P.; Di Stefano, L.; Di Meo, S. Oxidative stress in cold-induced hyperthyroid state; *J Exp Biol* **2010**, 213(Pt 17): 2899-2911. DOI 10.1242/jeb.043307.
52. Hunt, M.C.; Solaas, K.; Kase, B.F.; Alexson, S.E. Characterization of an acyl-coA thioesterase that functions as a major regulator of peroxisomal lipid metabolism; *J Biol Chem* **2002**, 277(2): 1128-1138. DOI 10.1074/jbc.M106458200。
53. Wang, J.; Wen, Y.; Zhao, W.; Zhang, Y.; Lin, F.; Ouyang, C.; Wang, H.; Yao, L.; Ma, H.; Zhuo, Y.; Huang, H.; Shi, X.; Feng, L.; Lin, D.; Jiang, B.; Li, Q. Hepatic conversion of acetyl-coA to acetate plays crucial roles in energy stress; *eLife* **2023**, 12. DOI 10.7554/eLife.87419.
54. Bajaj, R.; Rodriguez, B.L.; Russell, W.K.; Warner, A.N.; Diao, L.; Wang, J.; Raso, M.G.; Lu, W.; Khan, K.; Solis, L.S.; Batra, H.; Tang, X.; Fradette, J.F.; Kundu, S.T.; Gibbons, D.L. Impad1 and syt11 work in an epistatic pathway that regulates emt-mediated vesicular trafficking to drive lung cancer invasion and metastasis; *Cell Reports* **2022**, 40(13): 111429. DOI 10.1016/j.celrep.2022.111429.
55. Yang, Y. F.; Wang, Y.Y.; Hsiao, M.; Lo, S.; Chang, Y.C.; Jan, Y.H.; Lai, T.C.; Lee, Y.C.; Hsieh, Y.C.; Yuan, S.S.F. Impad1 functions as mitochondrial electron transport inhibitor that prevents ros production and promotes lung cancer metastasis through the ampk-notch1-hey1 pathway; *Cancer Letters* **2020**, 485: 27-37. DOI 10.1016/j.canlet.2020.04.025.
56. Lo, N.W.; Shaper, J.H.; Pevsner, J.; Shaper, N.L. The expanding beta 4-galactosyltransferase gene family: Messages from the databanks; *Glycobiology* **1998**, 8(5): 517-526. DOI 10.1093/glycob/8.5.517.
57. Rodeheffer, C.; Shur, B.D. Targeted mutations in beta1,4-galactosyltransferase i reveal its multiple cellular functions; *Biochim Biophys Acta* **2002**, 1573(3): 258-270. DOI 10.1016/s0304-4165(02)00392-6.
58. Youakim, A.; Dubois, D.H.; Shur, B.D. Localization of the long form of beta-1,4-galactosyltransferase to the plasma membrane and golgi complex of 3t3 and f9 cells by immunofluorescence confocal microscopy; *Proc Natl Acad Sci U S A* **1994**, 91(23): 10913-10917. DOI 10.1073/pnas.91.23.10913.